Ocean Sci. Discuss., doi:10.5194/os-2016-38, 2016
Manuscript under review for journal Ocean Sci.
Published: 27 June 2016

Ocean Science
Discussions
Open Access
EGU

Quality assessment of the TOPAZ4 reanalysis in the Arctic over the period 1991-2013

Jiping Xie[1], Laurent Bertino[1], Francois Counillon[1], Knut A. Lisæter[1], and Pavel Sakov[2]

[1]Nansen Environmental and Remote Sensing Center, Bergen N5006, Norway
[2]Bureau of Meteorology, Melbourne VIC3001, Australia

E-mail: jiping.xie@nersc.no

Abstract Long dynamical atmospheric reanalyses are widely used for climate studies, but data assimilative reanalyses of the Arctic ocean and sea ice are less common. TOPAZ4 is a coupled ocean and sea ice data assimilation system for the North Atlantic and the Arctic that is based on the HYCOM ocean model and the Ensemble Kalman Filter data assimilation method using 100 dynamical members. A 23-years reanalysis has been completed for the period 1991-2013. This study presents its quantitative quality assessment, compared to both assimilated and unassimilated observations available in the whole Arctic region in order to document the strengths and weaknesses of the system for potential users. It is found that TOPAZ4 performs well with respect to near surface ocean variables, but

Ocean Sci. Discuss., doi:10.5194/os-2016-38, 2016
Manuscript under review for journal Ocean Sci.
Published: 27 June 2016

some limitations appear in the interior of the ocean and for ice thickness, where observations are sparse. In the course of the reanalysis, the skills of the system are improving as the observation network becomes denser, in particular during the International Polar Year. The online bias estimation successfully maintains a low bias in our system.

Keywords: Arctic Ocean, Reanalysis, HYCOM, EnKF.

1. Introduction

The Arctic Ocean plays an important role in the global climate system, and in particular the sea ice at the interface between atmosphere and ocean regulates the fluxes of heat, moisture and momentum in ice-covered regions. The recent warming of the Arctic and the change of its water cycle has been linked to the following manifestations: a significant reduction and thinning of the sea ice cover (Johannessen et al., 2004; Shimada et al., 2006; Rothrock et al., 2008; Kwok and Rothrock, 2009); more freshwater in the Arctic in the 2000s (Haine et al., 2015); more mobility and faster deformations of the Arctic sea ice (Rampal et al., 2009; Spreen et al., 2011). The interpretation of such changes is severely hampered by the sparseness of the observations of sea ice and ocean, which is not expected to improve dramatically in a near future. It can be assisted by free-running model simulations, but those are usually hampered by the mislocation of the ice edge, of certain water masses in an unconstrained simulation. One then recurs to studying surrogate locations where similar processes are assumed to take place.

The latter activities thus necessitate state-of-the-art reanalysis databases able to honour accurately the observations in a physically consistent manner. Recent efforts in Arctic Ocean state estimation have delivered either long-

Ocean Sci. Discuss., doi:10.5194/os-2016-38, 2016
Manuscript under review for journal Ocean Sci.
Published: 27 June 2016

window optimizations (Nguyen et al., 2009, 2011) or more often short-window estimations (Schweiger et al., 2011; Mathiot et al., 2012; Sakov et al., 2012, Chevallier et al. 2016). Long-window optimizations deliver continuous model trajectories, which are physically more consistent than those using short windows. On the other hand, slicing the optimization problem into short windows makes the estimation problem more linear or better-conditioned (fewer unknowns and observations) and delivers more accurate products. Besides the window length, the choice of a background covariance matrix is also a critical aspect in a data-scarce area such as the Arctic. The background error covariance used in an ocean data assimilation system can be – by increasing order of complexity - based on fixed multivariate spatial statistics (Cummings et al., 2009), or an empirical estimation by a time-invariant ensemble (Oke et al., 2008) or a seasonally variable ensemble (Brasseur et al., 2005; Xie et al., 2011). In the case of ice-ocean systems, sea ice data assimilation often relies on rudimentary ice-only nudging methods (Schweiger et al., 2011; Tietsche et al., 2013), however the possibility to account for flow-dependent coupled ice-ocean data assimilation updates had already been demonstrated in Lisæter et al. (2003). The Pilot TOPAZ4 reanalysis of Sakov et al. (2012) has shown that the forecast error covariance from a dynamical ensemble was mitigating the physical inconsistencies that could be expected from a short assimilation window.

The TOPAZ4 system is a coupled ocean-sea ice data assimilation system of the physical environment in the North Atlantic and Arctic Ocean, which was initially used for short-term forecasting (Bertino and Lisæter, 2008) and later on for reanalysis (Sakov et al., 2012). TOPAZ4 represents the Arctic component of the MyOcean system (marine.copernicus.eu) where it is also

Ocean Sci. Discuss., doi:10.5194/os-2016-38, 2016
Manuscript under review for journal Ocean Sci.
Published: 27 June 2016

used with coupling to an ecosystem model (Samuelsen et al., 2015; Simon et al., 2015). The present paper follows the Pilot TOPAZ4 reanalysis by Sakov et al. (2012), which demonstrated the performance of the same system for the period of 2003-2008. They found that the EnKF data assimilation method can avoid ensemble collapse, and that the ensemble statistics provide reliable state-dependent error estimates and that data assimilation improves the match to independent observations compared to a free model.

TOPAZ4 system is forced by the ECMWF ERA Interim reanalysis (Dee et al., 2011) and assimilates most available measurements including along-track altimetry data, sea surface temperatures, sea ice concentrations and sea ice drift data from satellites as well as in situ temperature and salinity profiles. The proposed reanalysis is four times longer (1991-2013) than the pilot reanalysis and includes periods with poor observations and more intense observations efforts, such as during the International Polar Year (IPY, 2007-2009). The focus of this study is to provide a quantitative assessment of the performance of the reanalysis for ocean and sea ice variables in the pan-Arctic region (defined as north of 63°N) in order to guide the user about its skills and limitations. In particular, we investigate the variability of the performance in space, its seasonal cycle and its trend in the course of the reanalysis.

The outline of this paper is as follows: In section 2, the reanalysis system is described including the model, the data assimilation scheme, and the implementing set-up. Section 3 presents the result of against available observations: altimetry, SST, T-S profiles, ice concentration ice drift and ice thickness. For each of these quantities we assess variability of the performance of the system with space or with time. In Section 4, we

Ocean Sci. Discuss., doi:10.5194/os-2016-38, 2016
Manuscript under review for journal Ocean Sci.
Published: 27 June 2016

summarize the results, and discuss the results and the potential ways to improve our system for the next version of the reanalysis.

2. The reanalysis system

2.1 The HYCOM ice-ocean model

The TOPAZ4 system uses version 2.2 of the Hybrid Coordinate Ocean Model (HYCOM) developed at University of Miami (Bleck, 2002; Chassignet et al., 2003). The model is mainly unchanged compared to that used in Sakov et al. (2012). It uses 28 hybrid z-isopycnal layers, and the top layer has a minimum thickness of 3 m. The model grid has a horizontal resolution of 12-16 km, which is eddy permitting from the Equator to the Nordic Seas but is still far from being eddy-resolving in the Arctic. The lateral boundaries of temperature and salinity are relaxed to a combination of the World Atlas of 2005 (WOA05, Locarnini et al., 2006) and the version 3.0 of the Polar Science Center Hydrographic Climatology (PHC, Steele et al., 2001). HYCOM is coupled to a sea ice model in which the ice thermodynamics are described in Drange and Simonsen (1996) and the elastic-viscous-plastic rheology in Hunke and Dukowicz (1997). The surface momentum fluxes use a bulk formula parameterization (Kara et al. 2000), and the related thermodynamic fluxes are computed as described in Drange and Simonsen (1996).

The model has been initialized from the same climatology data as used at the boundaries. The model is spin up from 1973 using the European Center for Medium-Range Weather Forecast (ECMWF) ERA-Interim reanalysis data (Simmons et al., 2007). The Pacific water inflow is imposed by a barotropic inflow through the Bering Strait at the model boundary and balanced by an out flow at the southern boundary of the domain. Unlike in Sakov et al. (2012), the

Ocean Sci. Discuss., doi:10.5194/os-2016-38, 2016
Manuscript under review for journal Ocean Sci.
Published: 27 June 2016

inflow varies seasonally as found in observations (Woodgate et al., 2005): with a maximum in June (1.3 Sv), a minimum in January (0.4 Sv), and the mean transport of 0.8 Sv.

2.2 Data assimilation with the EnKF

Given observations, a model forecast, and assumptions on their respective uncertainties and at time t_i, the analyzed model state and its uncertainty can be computed by data assimilation using the least squares minimization (Evensen, 1994, 2003):

$$\mathbf{X}_i^a = \mathbf{X}_i^f + \mathrm{K}_i(\mathbf{d_i} - \mathbf{H}\mathbf{X}_i^f) \quad (1)$$

Where $\mathbf{d_i}$ is the observation vector, $\mathbf{X}_i$ is the model state vector and **H** is the observation operator denoting the projection from the model state variables to the measurement. The superscripts "a" and "f" refer respectively to the analyzed and the forecast states. We use the Deterministic form of the EnKF (Sakov and Oke 2008). Compared to Sakov et al. (2012), the only modification is the removal of the 1% multiplicative inflation near the end of the reanalysis (January 2010), which becomes problematic when used with spatially varying observational network (Anderson et al, 2001). Hence, multiplicative inflation in absence of observation (such as in the interior of the Arctic Ocean) leads to an exponential increase of the spread, which combined with a multivariate update makes it very sensitive to bias in the observed variable. Satellite sea ice concentration interpret melt pond in model as open water, which are not considered in TOPAZ4. This bias in the observed variable, was leading to a degradation of the stratification in the Arctic. The bias estimation procedure has also been modified as explained below (see Section 2.4).

Ocean Sci. Discuss., doi:10.5194/os-2016-38, 2016
Manuscript under review for journal Ocean Sci.
Published: 27 June 2016

2.3 Assimilated observations

The observations assimilated into the TOPAZ4 system are the same types as those assimilated in Sakov et al. (2012) except for some updates in the data sources. They are the satellite Sea Surface Temperature (SST), along-track Sea Level Anomalies (SLA) from satellite altimeters, in situ temperature and salinity profiles, Sea Ice Concentration (ICEC) and low-resolution sea ice drift data from satellites. An overview of the observations used in the reanalysis is given in Table 1. The preprocessing, temporal averaging and observation errors are following the procedure described in Sakov et al. (2012).

The SST data are initially the 1° resolution Reynolds SST from NOAA (Reynolds and Smith, 1994), upgraded in June 1998 by the high-resolution OSTIA data (Stark et al, 2007) from UK Metoffice. The SLA data assimilated in this system are the delayed time product (vxxc), which is validated unfiltered and not sub-sampled along-track SLA data with a resolution of 7 km, by Collecte Localisation Satellites (CLS). Furthermore, the assimilated ICEC are from the Ocean & Sea Ice Satellite Application Facility (OSISAF). Before 19 June 2002, this product is derived from SSM/I at 25 km resolution, and later derived from ARMSR-E 89 GHz brightness temperature at 12.5 km resolution. In the last three years, the ICEC resolution has been upgraded to 10 km. The temperature and salinity profiles include Argo floats, Damocles Ice-Tethered Profiles (ITP) and a large collection of hydrographic cruise data, as described in Sakov et al. (2012). At the exception from Reynolds SST, all data sources are available through the MyOcean portal.

Ocean Sci. Discuss., doi:10.5194/os-2016-38, 2016
Manuscript under review for journal Ocean Sci.
Published: 27 June 2016

2.4 Bias estimation in the TOPAZ4 reanalysis

As described in Sakov et al. (2012), two bias fields (for SST and mean sea surface height (MSSH)) are estimated online by model state augmentation, so that the analysis state of Equation (1) is modified as:

$$\begin{pmatrix} \mathbf{X}_i^a \\ \mathbf{B}_i^a \end{pmatrix} = \begin{pmatrix} \mathbf{X}_i^f \\ \mathbf{B}_i^f \end{pmatrix} + \mathrm{K}_i(\mathbf{d_i} - \mathbf{H}\mathbf{X}_i^f + \mathbf{H}\mathbf{B}_i^f) \ , \quad (2)$$

where $\mathbf{B}_i^a$ represents the bias estimates at the analysis time. The initial biases for each ensemble member are homogeneous in space, uniformly distributed with random values. For the SST, the initial biases are taken in [-4, 4] °C. And for the MSSH, the initial biases are in [-0.6, 0.6] m.

The bias fields are updated according to the sample covariance from the forecast ensemble and do not evolve during model integration. To avoid a collapse of the bias ensembles, an adequate multiplicative inflation is used (2% for SLA and 6% for SST). The multiplicative inflation of bias did not handle well the changes of observations coverage and has been replaced in May 2006 by additive inflation of identical amplitude (here after calling the event E9), using an auto-regressive temporal process of order one. After several assimilation steps, the bias fields converge to temporally stable but spatially variable fields. Figure 2 shows the bias estimates at end of the reanalysis for the SSH and the SST in the Arctic region. The bias patterns compare well with those obtained in Sakov et al. (2012)[1]. There are small discrepancies because the bias is estimated at a different time - December 2009 in Sakov et al. (2012) instead of December 2013 here - and the bias estimation is the result of a longer estimation period for which the signal to

[1] Sakov et al. (2012) present the mean SSH bias while we show the SSH bias of opposite sign.

Ocean Sci. Discuss., doi:10.5194/os-2016-38, 2016
Manuscript under review for journal Ocean Sci.
Published: 27 June 2016

noise ratio is reduced. The RMSD using the online-bias corrected values are slightly lower than the bias estimate of the last analysis step (not shown). Although the static part of the bias would be better estimated thoretically at the last assimilation of the reanalysis, the online bias approach can handle errors in the trend from seasonal bias and adjusting the observational network. The online bias estimate is provided together with the model output from 1999. In the following validation sections, the online bias estimates $\mathbf{B}_\mathbf{i}^\mathbf{a}$ are used to offset the reanalysis state from that date.

In order to avoid inconsistencies between assimilation of SST and temperature profile, the SST bias is injected downwards into the model mixed layer and decays exponentially.

3. Quantitative accuracy

In this section, we investigate whether the accuracy of the reanalysis varies spatially, seasonally or interannually. Such information is necessary for potential users of the reanalysis product. It also pinpoints the model limitations that motivate further model developments. The model error is calculated from the daily averages of the ensemble mean and the observations. The misfits of bias and root mean square differences (RMSD) are calculated as described in Equations of (3) and (4):

$$\text{Bias} = \frac{1}{N}\sum_{i=1}^{N}(\mathbf{H_i}\overline{\mathbf{X}}_\mathbf{i}^\mathbf{f} - \mathbf{d_i} - \mathbf{HB}_\mathbf{i}^\mathbf{f}) \quad (3)$$

$$\text{RMSD} = \sqrt{\frac{1}{N}\sum_{i=1}^{N}(\mathbf{H_i}\overline{\mathbf{X}}_\mathbf{i}^\mathbf{f} - \mathbf{d_i} - \mathbf{HB}_\mathbf{i}^\mathbf{f})^2} \quad , \quad (4).$$

Where $\overline{\mathbf{X}}_\mathbf{i}^\mathbf{f}$ is the forecasted daily average from the ensemble mean, which is compared to the observations $\mathbf{d}_\mathbf{i}$ on the same day. N is the number of daily

Ocean Sci. Discuss., doi:10.5194/os-2016-38, 2016
Manuscript under review for journal Ocean Sci.
Published: 27 June 2016

averages available over the diagnostic period (like either 365 or 366 for yearly). For SST and SLA, the bias term of B_i^f is the online bias estimate ($B_i^f = B_{i-1}^a$). Error bars are used to represent the standard deviations of these quantities - i.e. the variability of the RMSD or bias estimate through the calculation period.

3.1 Sea Level Anomalies

The variability in the SLA reanalysis accuracy is evaluated in the Pan-Arctic region (defined to the North of 63°N, see Fig. 1). The spatial variability of the bias and RMSD, calculated over the whole reanalysis period (1993-2013), is shown to the top of Fig.3. The residual bias is mainly positive, with much smaller amplitude than the estimated bias (see Fig.2). Some positive bias features reach up to 6 cm along the sea ice edge in the Greenland Sea and south of the Baffin Bay. Except for the sea ice edge in the Greenland Sea, the high RMSDs of SLA over 10 cm match the areas of large bias shown in Fig. 2. The spatially averaged bias is 2.1 cm, and the RMSD is about 6.7 cm.

The yearly time series of the SLA misfits and the observation number are shown in the left column of Fig. 4. The number of assimilated observations evolves with the launch or completion of satellite missions. The number of observation increases in 2000 with the launch of the GEOSAT Follow On (GFO) mission. The missions of Topex, Jason 1 and Jason 2 do not contribute directly in the Pan-Arctic region as their inclination is 66°, unlike 70° for GFO. There is a low observation period in 2008-2009 with the end of GFO mission, follow by an increase in 2011 with Cryosat-2, a decrease in 2012 with the end of Envisat and an last increase with the Saral/AltiKa mission in

Ocean Sci. Discuss., doi:10.5194/os-2016-38, 2016
Manuscript under review for journal Ocean Sci.
Published: 27 June 2016

2013. From 1993 to 2013, the RMSD decreased gradually from 8 cm to less than 6 cm. The most notable change is the introduction of the bias estimation and its reset in 2006. Afterwards, the residual bias stabilizes around 1cm but remains positive. The RMSD reduces then gradually with the introduction of new and more accurate observations. The reduced altimeter constellation in 2008-2009 does not cause an increase of the errors. This demonstrates the advantage of assimilating multiple types of observations, as improved SSH may also be the result of improved SST, or temperature and salinity profiles. Meanwhile, the temporal standard deviation of the RMSD during the year (shown as the-half-error bar) also reduces from 1-2 cm to less than 1 cm, indicating the system is getting more stable with time.

The seasonal cycle of the accuracy is shown in the right column of Fig. 4. The SLA being masked by sea ice, the number of observations varies seasonally in opposition to the sea ice cover. There is some seasonality in the RMSD, ranging from 5.5 to 7 cm as a consequence of the seasonal spatial coverage. The residual bias is positive through of the whole year reaching a maximum in April. This may be explained as well by the seasonal sea ice coverage, but also by a possible underestimation of the thermal expansion. The standard deviations of the residual bias and RMSD have no visible seasonality.

3.2 Sea Surface Temperatures

The spatial distribution of the SST misfits during 1999-2013 is shown in the bottom panels of Fig. 3. Note that SST is also masked under sea ice, as done during assimilation. There are stripes of cold residual bias and high RMSD along the ice edge from the North of the Barents Sea until the South of the Greenland Sea. These are contradictory to the sea ice concentration

Ocean Sci. Discuss., doi:10.5194/os-2016-38, 2016
Manuscript under review for journal Ocean Sci.
Published: 27 June 2016

biases in the same areas in Section 3.4, where a cold bias corresponds with too little ice. The accuracy of SST observations near the ice edge is poor and relies on strong ad-hoc assumptions. Another salient feature is the warm bias (> 0.2 °C) North of Denmark Strait. It is known that the recirculation of Atlantic Water inflow there in TOPAZ4 is excessive as identified in *Lien et al. (2016)*. This pattern was also visible in the estimated bias (Fig 2., with an opposite sign), suggesting that the estimated bias account for most of the bias but that it still underestimates the true bias. An additional stripe of the cold residual bias and higher RMSD is clear along the Mohn's Ridge, also pointing to topographic steering issues. In the Barents Sea, a weak bias is noticeable. Besides these areas, most of the SST RMSD is lower than 0.5 °C. On averaged in the whole Arctic region, the SST RMSD is about 0.45 °C during the period 1999-2013.

The evolution of SST accuracy of the TOPAZ4 reanalysis is shown on the left column of Fig. 5, together with the number of observations. In June 1998, the coarse resolution Reynolds SST is swapped to the higher resolution OSTIA SST and the number of observations increases drastically. On average over the whole period 1991-2013, the SST RMSD is about 0.64 °C, and the bias -0.08 °C. In the first years, the SST RMSDs are initially about 1 °C but decrease gradually down to 0.8 °C before the switch to OSTIA in 1998. During that period, the model has a cold SST bias around -0.3 °C and a standard deviation of 0.1 °C. After the introduction of OSTIA SST in 1998, the SST bias settles down closer to zero, but a slight positive is still noticeable before 2011. The RMSD decreases rapidly below 0.6°C in 1998 as a direct consequence of the reduction of the bias and the more abundant observations. The RMSD continues to reduce and reaches a minimum in

Ocean Sci. Discuss., doi:10.5194/os-2016-38, 2016
Manuscript under review for journal Ocean Sci.
Published: 27 June 2016

2010 below 0.4°C. At that time, the ensemble spread was getting too small, and the system performance was too constrained by SST as can be seen on the standard deviation of RMSD. It was thus decided to increase artificially the SST observation errors, which resulted in a small increase of the error up to 0.5 °C. It is clear from the above that the transition to high-resolution SST in our system has led to higher SST accuracy.

Furthermore, the seasonal variability of the SST performance is shown in Fig. 5. As for SLA, the number of observations varies seasonally with the sea ice mask and causes changes of the bias and RMSD: the RMSD is minimum in September and October with less than 0.4 °C when there are more observation and is maximum over 0.6 °C in June and July when the bias is as well maximum. The reason for the larger bias in summer months is unclear but is possibly related to errors in the mixed layer depths and the atmospheric radiative forcing.

3.3 In situ temperature and salinity profiles

There are 1.1×10^5 temperature and salinity profiles assimilated in the Pan-Arctic region during the period 1991-2013, but the distribution of these profiles is very uneven both in time and space, with more observations in ice-free areas and during the IPY. The averaged assimilated temperature and salinity profiles, the corresponding profiles from the reanalysis, the climatology WOA13 (Locarnini et al., 2013) and their misfits are all shown in Fig.6. The stratification in the Arctic varies regionally, depending on the influence of the Atlantic Water inflow, the Pacific Water inflow and the river discharge. We have thus divided the analysis into four sub-regions: the central Arctic, the Barents Sea, the Greenland Sea, and the Norwegian Sea (see Fig.1).

Ocean Sci. Discuss., doi:10.5194/os-2016-38, 2016
Manuscript under review for journal Ocean Sci.
Published: 27 June 2016

In the central Arctic, the average profiles depict well the cold halocline water near the surface and warmer water and saline water around 400 m associated with Atlantic Water. In the near surface, TOPAZ4 is doing slightly better than the climatology for salinity. The core Atlantic Water is clearly too diffuse in TOPAZ4 (not pronounced enough and vertically too broad) leading to a cold bias (-0.3 °C) and RMSD (0.5 °C) around that depth. An area of larger RMSD is noticeable around 1000 m (0.6 °C and 0.3 psu). Since the bias at that depth is low and since climatology has lower RMSD, it suggests that TOPAZ4 has too much variability at depths. That variability is likely due to the data assimilation setup with the combined effect of multiplicative inflation and spurious correlations (see Section 2.2).

In the Greenland Sea, the temperature RMSDs and biases are again slightly better than the climatology near the surface (upper 200m), but degrade very near below, reaching the maxima of RMSD (> 1 °C and 0.1 psu) and bias around 800m.

In the Norwegian Sea, the features are similar: the model having some skills near the surface but deteriorating at depths. The Atlantic Water (AW) is present but it is too diffuse. It is too broad and does not capture the maximum at the same depth as in the observation. It is a well-known limitation of ocean models nowadays (Ilicak et al., 2016).

In the Barents Sea, the RMSD for temperature and salinity is improved near surface, compared to the climatology. But the AW (temperature > 3°C and salinity > 35 psu, Blindheim and Østerhus, 2003) of the TOPAZ4 is too warm and saline, which suggests there is too much AW inflow or too weak vertical mixing.

Ocean Sci. Discuss., doi:10.5194/os-2016-38, 2016
Manuscript under review for journal Ocean Sci.
Published: 27 June 2016

In Fig. 7, the evolution of the performance of TOPAZ4 for temperature and salinity is presented by the time series of innovation diagnostics at depths of 300-800 m. The system performance is relatively stable until 2006, with a cold and fresh bias and RMSD of about 1.5°C and 0.1 psu. From 2006, the performance is greatly improved, supposedly by the combined effect of the change from multiplicative to additive inflation and with the large increase of observation number during the international Polar Year (IPY) period. Once the IPY period is finished, the number of observation drastically reduces. It results in a clear increase of the RMSD and bias for temperature to a level intermediate to prior the IPY period, but the error for salinity remains to a lower level than before the IPY.

3.4 Sea ice concentration

Relative to the daily sea-ice concentration product from OSISAF (Copernicus OSI TAC product), the spatial variability of the daily misfits of sea-ice concentration is shown in Fig.8. As there is a large seasonal variability in the sea-ice extent, this is carried out at two characteristic times of one year: the maximum (March) and minimum ice extent (September).

In March, there is a dipole anomaly on either sides of the ice edge in the Greenland Sea. The ice edge in TOPAZ4 is transiting too sharply from pack ice to open water, because the heat capacity of the ice is neglected. This leads to a dipole bias (positive inside the ice and negative outside) during the melting season. There is also a weak bias over regions that are usually ice-free. Indeed, OSISAF does not employ weather filtering and places a thick band of low concentration (< 10%) in ice-free region (Ivanova et al. 2015).

Ocean Sci. Discuss., doi:10.5194/os-2016-38, 2016
Manuscript under review for journal Ocean Sci.
Published: 27 June 2016

In September, TOPAZ4 shows a negative bias in the Greenland Sea. At that time of the year, the sea ice flows southwards and TOPAZ4 tends to underestimate the southern extension of the sea ice tongue along Greenland. This indicates that the dynamical forcing is biased or that the drag coefficients are incorrect as the ice is in free drift there.

The RMSD is approximately 5% in the whole of Arctic region, which is good in view the accuracy of the data set (~10%). There are regions where the RMSD exceeds 25%, which coincides with regions where the bias is high. Data assimilation does constrain the sea ice concentrations but the model biases (lack of resolution of ocean currents, biases of ice drift or ice thickness) still cause locally high residual errors of ice concentrations.

In order to assess the interannual variability of the performance of TOPAZ4, we have decided to use the standard sea-ice extent (SIE) metric. SIE is calculated as the surface area in which the ice concentration is larger than 15 %.

As the variability in the decadal trend of SIE in the Arctic is large, we present the interannual evolution in the whole Arctic and in two sub-regions: the Greenland Sea and Barents Sea (Fig. 9). TOPAZ4 shows good agreement with the OSISAF observations in the Pan-Arctic region and the mean SIE in the 23 years are 8.03×10^6 instead of 7.96×10^6 km^2 in the observations. The decreasing trend of the SIE during the period 1991-2013, is -6.16×10^4 $km^2\ y^{-1}$, which compares well to the trend of the observations (-6.34×10^4 $km^2\ y^{-1}$).

In the Greenland Sea, the SIE in TOPAZ4 is underestimated, which clearly relate the bias in the southern extent of the sea-ice tongue along the coast of Greenland. The bias in TOPAZ4 is in averaged -3.6×10^4 km^2 and the decreasing trend in TOPAZ4 is -3.1×10^3 $km^2\ y^{-1}$, which is larger than observed

Ocean Sci. Discuss., doi:10.5194/os-2016-38, 2016
Manuscript under review for journal Ocean Sci.
Published: 27 June 2016

(-2.3x10^3 km^2 y^{-1}). In the Barents Sea, the variability agrees well, although TOPAZ4 underestimates slightly the SIE. The decreasing trend is comparable. The seasonality of the SIE in OSISAF and TOPAZ4 are investigated in Fig. 10. It is clear that the seasonal cycle of the ice extent is generally well simulated by the reanalysis in the Pan-Arctic area. In the summer months from June to August, a little underestimation of the extent in the reanalysis is apparent, and the minimal ice extent is a little early compared to the observations. In the Greenland Sea, the underestimation feature of sea ice extent is large. The underestimation of sea ice extent starts in February and increases during the sea ice melt, reaching a maximum (of about 1x10^5 km^2) in July. In the Barents Sea, the seasonal cycle is well simulated but some differences are noticeable there in the beginning of the year, reaching a maximum in April, but close to zero in August and September when there is no ice.

3.5 Sea Ice Drift

The sea ice drift from the buoy data of the International Arctic Buoy Probram (IABP) are available at 12h frequency from 1991 to 2011,is an independent data set and is used here for validation. To avoid the “survival bias” caused by the retreat of sea ice from the marginal seas and unresolved coastal effects, the buoy drift vectors are limited to the central Arctic, as shown with the red line in the right panel of Fig. 1. The waters shallower than 30 m and closer than 50 km from the coastline are excluded. This data set has been gridded to be compared with the model. Each grid cell is filled (i.e. considered reliable) if the calculation involves at least 30 buoys within a day. A coarser grid than the model resolution is used (4 grid cells which corresponds to approximately

Ocean Sci. Discuss., doi:10.5194/os-2016-38, 2016
Manuscript under review for journal Ocean Sci.
Published: 27 June 2016

60x60 km^2) to avoid having too many empty cells. The daily averaged from the measurement is the mean of the 12h drifting speed. For comparison, the model drifting speed is calculated from daily averaged of eastward and northward velocity. Several approximations are made during this comparison; we compare Eulerian with lagrangian drift for which the drift is expected to be larger; the model ice drift is calculated from daily average of u and v instead of daily ice drift for which the drift is higher by approximately 0.5 km per day (not shown).

On averaged over the period 1991-2011, the mean drift fields of sea ice are presented in Fig. 11. As the resulting drift estimate appeared noisy, we have applied a smoothing with the neighboring grid cells. Both observations and TOPAZ4 show similar pattern with a pronounced Beaufort Gyre, although the center of the Gyre differs slightly. We can also notice that TOPAZ4 overestimates globally the ice drift with a bias of 1.7 km d^{-1}. In the Chukchi Sea, TOPAZ4 underestimates the drift by approximately -2 km d^{-1}.

Over the period 1991-2011, the monthly time series of the Ice drift speeds are compared in Fig. 12. They are averaged in the Central Arctic from the reanalysis and the buoy data respectively. On average, the drift speed is about 7 km d^{-1} in buoy data, and about 9.4 km d^{-1} in TOPAZ4 reanalysis. The fast bias is clear until the end of 2010. From that time, the drag coefficient of the atmosphere on sea-ice has been reduced from 2.14×10^{-3} to 1.6×10^{-3}. We can see that the bias is much reduced during the last year. The RMSD is on average 5.1 km d^{-1}, of which 2.5 km d^{-1} can be attributed to the bias. The correlation between the 2 curves is about 0.6. In addition, the monthly seasonality anomaly of the ice drift for the period 1991-2011 is plotted in Fig. 13. While the buoys show a clear seasonality in the ice drift, being slowest in

Ocean Sci. Discuss., doi:10.5194/os-2016-38, 2016
Manuscript under review for journal Ocean Sci.
Published: 27 June 2016

March and fastest in September, the seasonality in TOPAZ4 reanalysis is weaker and reaches a minimum in May (delayed by 2 months).

3.6 Sea ice thickness

The sea ice thickness in Arctic has been paid much attention in recent years because it has been found to be sensitive to global warming (Kwok et al., 2009; Zygmuntowska et al., 2014). In this study, sea ice thickness is an independent data set, as it has not been assimilated. The observations of ice thickness are yet very few. A satellite-derived product for the Arctic Ocean ice provides the estimations of sea ice thickness for February-March and October-November between 2003-2008 (ICESat, Kwok et al., 2009). Figure 14 shows the spatial distributions of the mean sea ice thicknesses and their differences. The spatial correlations are 0.74 and 0.87 for spring and fall, respectively. On average, TOPAZ4 is too thin compared to ICESat with a bias of -0.79 m and -0.64 m, in spring and in fall. In spring, TOPAZ4 is too thin, in particular north of Ellesmere Island by approximately 2 m. There is a positive bias centered in the Beaufort Gyre in spring. In fall this bias is wider and displaced slightly to the east.

Another source of validation is the Unified Sea Ice Thickness Climate Data Record (Lindsay, 2013) resulting from a concerted effort to collect as many observations as possible of Arctic sea-ice draft, freeboard, and thickness. The sea ice draft is measured by Sonar of US Navy Submarines from National Snow and Ice Data Center (USSUB-DG and USSUB-AN, Wadhams and Horne, 1980; Wensnahan and Rothrock, 2005; Rothrock and Wensnahan, 2007), and the sea ice thickness by flight campaigns from NASA Operation IceBridge (IceBridge, Kurtz et al., 2013), as shown in Fig. 15(a). The sea-ice

Ocean Sci. Discuss., doi:10.5194/os-2016-38, 2016
Manuscript under review for journal Ocean Sci.
Published: 27 June 2016

draft data has been diagnosed in TOPAZ4 as proposed by the equation (4) of Alexandrov et al. (2010):

$$D_i = H_i \cdot \frac{\rho_i}{\rho_w} + H_{sn} \cdot \frac{\rho_{sn}}{\rho_w} \quad (5).$$

Where D_i is ice draft, H_i is ice thickness, and H_{sn} is the snow thickness. The ρ_i, ρ_w, and ρ_{sn} are the densities for ice, water, and snow (respectively 900 kg m^{-3}, 1000 kg m^{-3}, and 300 kg m^{-3}).

The IceBridge ice thickness covers the period of 2009-2011. TOPAZ4 reanalysis is too thin with a bias of 1.1 m, a RMSD of 1.4 m and a correlation of 0.5. The bias against the sea ice draft is smaller with 0.3-0.4 m, and a RMSD about 0.6-0.7 m. The correlation coefficients are relatively good with .86 and 0.69, which is higher than for the IceBridge data. These discrepancies are likely to be related to the spatial distribution of the different data set. Hence, IceBridge data is concentrated around the Northern coast of Greenland where TOPAZ4 showed largest bias in the comparison with ICESAT.

As another diagnostics of interest, the daily time series of sea ice volume from TOPAZ4 in the Arctic of 1991-2013 is shown by the blue curve in the left panel of Fig. 16. Before 2001, the sea ice volume varies stably around 1.4×10^4 km^3, with a significant seasonal variability between 8×10^3 km^3 and 1.9×10^4 km^3. Afterwards in the period 2001-2010, the sea ice volume decreases dramatically. This reduction of sea ice volume is qualitatively consistent with the limited satellite records. First the estimate from Kwok et al. (2009), derived from the ICESat record from 2003 to 2008, shows a similar trend. After revising the uncertainties of input data (snow depth, sea ice density and ice concentrations), Zygmuntowska et al. (2013) corrected the

Ocean Sci. Discuss., doi:10.5194/os-2016-38, 2016
Manuscript under review for journal Ocean Sci.
Published: 27 June 2016

estimates of the mean sea ice volume, shown as the starred line in Fig. 16. With respect to these sea ice volume estimates, TOPAZ4 still has too little ice. In the right panel of Fig. 16, the seasonal cycles of sea ice volume from TOPAZ4 and the standard deviation in the 23 years are shown by the blue curve and the cyan error bars respectively. In May, the maximum sea ice volume is about $1.5x10^4$ km^3, and in September is less than $5x10^3$ km^3. The sea ice volumes from Zygmuntowska et al. (2013) are plotted on top of the averaged TOPAZ4 seasonal cycle in the period 1991-2013. These correspond well to the model climatology, but still betray an underestimation because the measurements are representative of a period of lower ice volume. The TOPAZ4 seasonal cycle of ice volume seems to change in amplitude during different time eras, although the reasons lie in two successive changes of the settings of the EnKF. In December 2001, the variance of precipitation errors is increased from 1.10^{-17} to 1.10^{-12} $m^2.s^{-2}$, as an adjustment for a slow decrease of ensemble spread. These perturbations being truncated Gaussian, the truncation resulted in excessive snow precipitations. The excessive snow depths has then isolated the ice from the atmosphere and reduced the amplitude of the yearly cycle from 1.08 m to 0.74 m (see Figure 17), this also delayed the phase of the cycle. In January 2011, an unbiased log-normal law replaces the truncated Gaussian perturbations with an amplitude of 30%. The amplitude and phase of the seasonal cycle return to more correct values. The sensitivity experiments in Finck et al. (2013) verified the above-mentioned issue.

4. Summary and discussions

The above findings can be summarized variable by variable:

Ocean Sci. Discuss., doi:10.5194/os-2016-38, 2016
Manuscript under review for journal Ocean Sci.
Published: 27 June 2016

- **SLA:** In the period 1993-2013, the RMSD of daily SLA in the reanalysis is gradually decreased from near 8 cm to less than 6 cm in the Pan-Arctic region. The introduction of a bias estimation scheme proves very efficient in constraining the bias. The largest RMSDs over 10 cm are found in the Lofoten Basin. There is also a patch of larger error near the ice edge, but observations are also less accurate there. There is a weak seasonality in the performance of the system with the best in summer months.
- **SST:** The SST RMSD is about 0.66 °C, and the bias is about 0.04 °C. Some biases along the sea-ice edge can be related to errors in the observations. Other biases and RMSD relate to errors in the circulation within the Nordic Sea. The transition to OSTIA high-resolution observation is highly beneficial for constraining the bias and the RMSD, but an overestimation of the observation error from the provider was needed to avoid a collapse of the ensemble spread. The performance of the system varies seasonally following the amount of observations and a larger bias during summer months.
- **Temperature and salinity profiles:** The errors are lower than the WOA13 climatology near the surface (in the top of 100 to 200 m). Below this depth, the model shows large biases and performs poorer (RMSD > 1°C and about 0.1 psu). Some of the biases relate to the limitations of the model to maintain the Atlantic water (as expected from Ilicak et al. 2016) and others relate to a degradation introduced by data assimilation (a flat multiplicative inflation). A large improvement occurs at the time when the inflation method was replaced and when more numerous observations were available from the IPY.

Ocean Sci. Discuss., doi:10.5194/os-2016-38, 2016
Manuscript under review for journal Ocean Sci.
Published: 27 June 2016

- **Sea ice concentration and extent:** TOPAZ4 agrees well with the OSI-SAF sea ice concentrations. On average, the RMSDs are lower than 5% and the biases close to zero. The errors are larger close to the ice edge, and poorest in the Greenland Sea. The errors are related to biases in the thermodynamics and dynamics of the sea-ice model. The bias is largest during the summer season. The performance is stable throughout the reanalysis.
- **Sea ice drift:** The averaged drift in TOPAZ4 shows comparable patterns to independent observation from IAPB buoys with the classical Beaufort Sea gyre and transpolar drift. However the center of the gyre is slightly misplaced. The RMSD of drift speed in the reanalysis is about 5.1 km d^{-1}, and has a fast bias by about 2.5 km d^{-1}. The monthly time variability compares well, but TOPAZ4 has a too weak seasonal cycle and shifted by two months. From 2011 onwards, the atmospheric drag coefficient was adjusted and the ice drift speed agrees better with observations after the change. Still, with RMSDs of 5 km d^{-1} close to the signal itself, improving the performance of ice drift appears as a priority for future operational use.
- **Sea ice thickness:** TOPAZ4 shows some large biases (approximately -1.1 m) compared to ice thickness from ICESat and IceBridge as well as compare to ice draft data. The bias is largest north of Ellesmere Island with bias up to 2 m. The spatial pattern and regression compare reasonably well. The ice is too thin in the period 2001-2010 due to excessive snow depths and the seasonal cycle is too small during that time.

Ocean Sci. Discuss., doi:10.5194/os-2016-38, 2016
Manuscript under review for journal Ocean Sci.
Published: 27 June 2016

The results from the 23-years reanalysis show overall a good stability and good agreements with observations. However assessing the system for such a long period also reveals some limitations that are inherent to the data assimilation method or due to model flaws. In the following, we illustrate the possible reasons and the means to tackle these in the future version of TOPAZ5 system.

- The Atlantic Waters have a too diffuse signature. In order to improve their advection, we will double the horizontal and vertical resolution (58 hybrid layers and 5 km horizontal resolution). The parameterization of diapycnal mixing will be reduced under sea-ice as proposed in Morison et al. (1985). We also foresee that increasing the resolution will improve the circulation in the Nordic Seas and reduce the associated biases of SST and SSH.
- The system has a too sharp ice edge. The current thermodynamic model does not account for the heat capacity of the sea-ice. TOPAZ5 will transit to the community sea-ice mode CICE (Hunke et al. 2010), which uses an improved thermodynamic parameterization.
- Observations detect melt ponds as open water, whereas melt ponds are not simulated in the current TOPAZ4. This creates bias in sea-ice during summer months that is transferred to the interior of the ocean via coupled data assimilation. In the future, we will choose the best alternative between using an existing melt pond model or detect and remove the signature of the melt ponds from the observations.
- Comparisons against sea-ice drift and ice thickness highlighted more severe limitations: Too thin ice, a too smooth thickness gradient from Greenland into the Beaufort Gyre; the center of the Beaufort Gyre

Ocean Sci. Discuss., doi:10.5194/os-2016-38, 2016
Manuscript under review for journal Ocean Sci.
Published: 27 June 2016

being slightly misplaced, the sea-ice drift being too fast. These biases can be reduced by optimizing the sea ice strength (P*) and the atmospheric and ocean drag parameters (Massonnet et al. 2014). However, optimal values of these parameters are moving targets in view of their limited physical realism. The methodology proposed by Barth et al. (2015), to estimate biases in atmospheric wind from ice drift will also be considered. But the RMSDs of ice drift are relatively high (5 km d^{-1} for an ice drift generally inferior to 10 km d^{-1}) although comparable to short-term forecasts in Schweiger and Zhang (2015). These fluctuating errors are less likely to be reduced by model tuning.

- There are further indications that the viscous-plastic and the related elastic-viscous-plastic rheologies have inherent limitations for simulating long-term properties of the ice drift – e.g. the acceleration of sea ice drift, the phase of its seasonal cycle (Rampal et al. 2011). A high-priority objective is therefore to couple TOPAZ to the neXtSIM sea-ice model that is based on an elasto-brittle rheology. Recent studies with forced version of neXtSIM (Bouillon and Rampal, 2015; Rampal et al., 2016) suggest that the model is capable of reproducing the sea ice deformations over a wide range of spatial and temporal scales and reduces the error of the sea ice drift. It is of interest to understand to which extent the coupling feedback will respond to this improved dynamical model.
- The online bias estimation appeared quite successful to limit bias in our model, but its implementation in the EnKF was very sensitive to the choice of inflation method used. The present configuration that combined r-factor inflation and autoregressive additive inflation is our

Ocean Sci. Discuss., doi:10.5194/os-2016-38, 2016
Manuscript under review for journal Ocean Sci.
Published: 27 June 2016

recommendation in a realistic system with a highly spatially variable observation network.

- The EnKF has proven capable to assimilate a large variety of observations, but more observations should be added. The sea-ice thickness of thin ice from the European Space Agency's (ESA) Soil Moisture and Ocean Salinity (SMOS) in Kaleschke et al. (2012) and Tian-Kunze et al. (2014). Also the complementary thickness of thick ice from ICESat (Kwok et al. 2009) and CryoSat-2 (Wingham et al., 2006; Laxon et al., 2013), and SMOS sea surface salinity (Reul et al., 2012).

Acknowledgements

Thanks to Dr. P. Rampal for processing the buoy dataset for sea ice drift and useful discussions. This study was supported by successive MyOcean projects from the European Commission (Grant numbers 218812), the Arctic element of the Copernicus Marine Services and a grant of CPU time from the Norwegian Supercomputing Project (NOTUR II grant number nn2993k).

References

Alexandrov, V., S. Sandven, J. Wåhlin, and O.M. Johannessen, 2010: The relation between sea ice thickness and freeboard in the Artic. The Cryosphere 4: 378-380. doi: 10.5194/tc-4-373-2010.

Anderson, J. L., 2001: An ensemble adjustment Kalman filter for data assimilation. Mon. Wea. Rev. 129, 2884-2903, DOI: http://dx.doi.org/10.1175/1520-0493(2001)129<2884:AEAKFF>2.0.CO;2.

Ocean Sci. Discuss., doi:10.5194/os-2016-38, 2016
Manuscript under review for journal Ocean Sci.
Published: 27 June 2016

Barth, A., M. Canter, B. V. Schaeybroeck, et al., 2015: Assimilation of sea surface temperature, sea ice concentration and sea ice drift in a model of the Southern Ocean." *Ocean Modelling,* 93(9), 22-39, doi:10.1016/j.ocemod.2015.07.011.

Bertino, L. and K. A. Lisæter, 2008: The TOPAZ monitoring and prediction system for the Atlantic and Arctic Oceans, Journal of Operational Oceanography, 1(2), 15–19, doi: 10.1080/1755876X.2008.11020098.

Bleck, R., 2002: An oceanic general circulation model framed in hybrid isopycnic-Cartesian coordi- nates, Ocean Model., 4, 55–88, doi:10.1016/S1463-5003(01)00012-9.

Blindheim, J., and S. Østerhus, 2003: The Nordic Seas, Main Oceanographic Features. In: The Nordic Seas: An Integrated Perspective, in: Drange, H., Dokken, T., Furevik, T., Gerdes, R., Berger, W. (Eds.), Amer. Geophys. Union Mono. Ser. 158, 11-37.

Brasseur, P., P. Bahurel, L. Bertino, F. Birol, J. -M. Brankart, N. Ferry, S. Losa, E. Remy, J. Schröter, S. Skachko, C. -E. Testut, B. Tranchant, P. J. Van Leeuwen, and J. Verron, 2005: Data assimilation for marine monitoring and prediction: The MERCATOR operational assimilation systems and the MERSEA developments, Q. J. R. Meteorol. Soc., 131(613), 3561– 3582, doi: 10.1256/qj.05.142.

Bouillon, S., and P. Rampal, 2015: Presentation of the dynamical core of neXtSIM, a new sea ice model. *Ocean Modelling*, 91(7), 23-37, doi:/10.1016/j.ocemod.2015.04.005.

Chassignet, E. P., L. T. Smith, and G. R. Halliwell, 2003: North Atlantic Simulations with the Hybrid Coordinate Ocean Model (HYCOM): Impact of the vertical coordinate choice, reference pressure, and termobaricity, J. Phys. Oceanogr., 33, 2504–2526, Doi:http://dx.doi.org/10.1175/1520-0485(2003)033<2504:NASWTH>2.0.CO:2.

Chevallier, M., D. Salas-Mélia, A. Voldoire, and M. Déqué, 2013: Seasonal forecasts of the Pan-Arctic sea ice extent using a GCM-based seasonal prediction system.

Ocean Sci. Discuss., doi:10.5194/os-2016-38, 2016
Manuscript under review for journal Ocean Sci.
Published: 27 June 2016

J. Climate, 26, 6092-6104, DOI: http://dx.doi.org/10.1175/JCLI-D-12-00612.1.

Chevallier, M., G. C. Smith, F. Dupont, and J. -F. Lemieux et al., 2016: Intercomparison of the Arctic sea ice cover in global ocean–sea ice reanalyses from the ORA-IP project. Climate Dynamics, 10.1007/s00382-016-2985-y.

Cummings, J., L. Bertino, P. Brasseur, I. Fukumori, M. Kamachi, M. Martin, K. Mogensen, P. Oke, C. E. Testut, J. Verron, and A. Weaver, 2009: Ocean data assimilation systems for GODAE, Oceanography, 22 (3), 96–109, http://dx.doi.org/10.5670/oceanog.2009.69.

Dee, D.P., S. M. Uppala, A. J. Simmons, P. Berrisford, et al., 2011: The ERA-Interim reanalysis:configuration and performance of the data assimilation system, Quart. J. Roy. Meteor. Soc., 137, 553–597, Doi: 10.1002/qj.828.

Drange, H., and K. Simonsen, 1996: Formulation of air-sea fluxes in the ESOP2 version of MICOM, Technical Report No. 125 of Nansen Environmental and Remote Sensing Center, 23pp.

Evensen, G., 1994: Sequential data assimilation with a nonlinear quasi-geostrophic model using Monte Carlo methods to forecast error statistics. J. Geophys. Res., 99, 10143–10162, doi: 10.1029/94JC00572.

—, 2003: The ensemble Kalman filter: theoretical formulation and practical implementation. Ocean Dynamics, 53, 343–367, doi: 10.1007/s10236-003-0036-9.

Finck, N., F. Counillon, L. Bertino, S. Bouillon, and P. Rampal, 2013: Validation of sea ice quantities of TOPAZ for the period 1990-2010. Technical Report No. 332 of Nansen Environmental and Remote Sensing Center, 30pp.

Haine, T., B. Curry, R. Gerdes, E. Hansen, M. Karcher, C. Lee, B. Rudels, G. Spreen, L. Steur, K. D. Stewart, and R. Woodgate, 2015: Arctic freshwater export: Status, mechanisms, and prospects. Global and Planetary Change, 125, 13-35, doi: 10.1016/j.gloplacha.2014.11.013.

Hunke, E. C. and J. K. Dukowicz, 1997: An elastic-viscous-plastic model for sea ice dynamics, J. Phys. Oceanogr., 27, 1849–1867, Doi:

http://dx.doi.org/10.1175/1520-0485(1997)027<1849:AEVPMF>2.0.CO:2.

Hunke, E. C., W. H. Lipscomb, and A. K. Turner, 2010: CICE: the Los Alamos Sea Ice Model Documentation and Software User's Manual Version 4.1 LA-CC-06-012, *T-3 Fluid Dynamics Group, Los Alamos National Laboratory, Los Alamos NM 87545,* 76pp.

Ilicak, M., H. Drange, H. Wang et al., 2016: An assessment of the Arctic Ocean in a suite of interannual CORE-II simulations. Part III: Hydrography and fluxes. Ocean Modelling. 100, 141-161, doi:10.1016/j.ocemod.2016.02.004.

Ivanova N. et al, 2015. Ivanova, N., L. T. Pedersen, R. T. Tonboe, S. Kern, G. Heygster, T. Lavergne, A. Sørensen, R. Saldo, G. Dybkjær, L. Brucker, et al., 2015: Inter-comparison and evaluation of sea ice algorithms: towards further identification of challenges and optimal approach using passive microwave observations. The Cryosphere, 9(5), doi: 10.5194/tcd-9-1269-2015.

Johannessen, O. M., L. Bengtsson, M. W. Miles, S. I. Kuzmina, V. A. Semenov, G. V. Alekseev, A. P. Nagurny, V. F. Zakharov, L. P. Bobylev, L. H. Pettersson, K. Hasselmann, and H. P. Cattle, 2004: Arctic climate change - observed and modelled temperature and sea-ice variability, Tellus A, 56 (4), 328-341, doi:10.1111/j.1600-0870.2004.00060.x.

Kaleschke, L., X. Tian-Kunze, N. Maaß, M. Mäkynen, and M. Drusch, 2012: Sea ice thickness retrieval from SMOS brightness temperatures during the Arctic freeze-up period. J. Geophys. Lett. 39, L05501, doi: 10.1029/2012GL050916.

Kara, A., P. A. Rochford, and H. E. Hurlburt, 2000: Efficient and accurate bulk parameterizations of air-sea fluxes for use in general circulation models, J. Atmos. Oceanic Technol, 17, 1421– 1438, DOI: http://dx.doi.org/10.1175/1520-0426(2000)017<1421:EAABPO>2.0.CO;2.

Karl, T. R., A. Arguez, B. Huang, J. H. Lawrimore, J. R. McMahon, M. J. Menne, T. C. Peterson, R. S. Vose, and H. -M. Zhang, 2015: Possible artifacts of data biases in the recent global surface warming hiatus. Science, 348 (6242), 1469-1472, doi:

10.1126/science.aaa5632.

Kurtz, N. T., S. L. Farrell, M. Studinger, N. Galin, J. P. Harbeck, R. Lindsay, V. D. Onana, B. Panzer, and J. G. Sonntag, 2013: Sea ice thickness, freeboard, and snow depth products from Operation IceBridge airborne data. The Cryosphere, 7, 1035-1056. doi:10.5194/tc-7-1035-2013.

Kwok, R., G. F. Cunningham, M. Wensnahan, I. Rigor, H. J. Zwally, and D. Yi, 2009: Thinning and volume loss of the Arctic Ocean sea ice cover: 2003-2008, J. Geophys. Res., 114, C07005, doi: 10.1029/2009JC005312.

Kwok, R., and D. Rothrock, 2009: Decline in Arctic sea ice thickness from submarine and ICESat records: 1958–2008, Geophys. Res. Lett., 36, L15501, doi:10.1029/2009GL039035.

Laxon, S. W., K. A. Giles, A. L. Ridout, D. J. Wingham, et al., 2013: CryoSat-2 estimates of Arctic sea ice thickness and volume, Geophys. Res. Lett., 40, 732–737, doi:10.1002/grl.50193.

Lien, V. S., S. S. Hjøllo, M. D. Skogen, E. Svendsen, H. Wehde, L. Bertino, F. Counillon, M. Chevallier, and G. Garric, 2016: An assessment of the added value from data assimilation on modelled Nordic Seas hydrography and ocean transports, Ocean Modelling, doi:10.1016/j.ocemod.2015.12.010.

Lindsay, R. W., 2013: Unified sea ice thickness climate data record collection spanning 1947-2012. Boulder, Colorado USA: National Snow and Ice Data Center. http://dx.doi.org/10.7265/N5D50JXV.

Lisæter, K., J. Rosanova, and G. Evensen, 2003: Assimilation of ice concentration in a coupled ice-ocean model, using the Ensemble Kalman filter, Ocean Dynam., 53, 368–388, doi: 10.1007/s10236-003-0049-4.

Locarnini, R., J. Antonov, and H. Garcia, 2006: World Ocean Atlas 2005, Volume 1: Temperature., vol. 61, US Dept. of Commerce, National Oceanic and Atmospheric Administration.

Locarnini, R. A., A. V. Mishonov, J. I. Antonov, T. P. Boyer, H. E. Garcia, O. K.

Ocean Sci. Discuss., doi:10.5194/os-2016-38, 2016
Manuscript under review for journal Ocean Sci.
Published: 27 June 2016

Baranova, M. M. Zweng, C. R. Paver, J. R. Reagan, D. R. Johnson, M. Hamilton, and D. Seidov, 2013: World Ocean Atlas 2013, Volume 1: Temperature. In S. Levitus and A. Mishonov, editors, NOAA Atlas NESDIS, 40 pp.

Massonnet, F., H. Goosse, T. Fichefet, and F. Counillon, 2014: Calibration of sea ice dynamic parameters in an ocean-sea ice model using an ensemble Kalman filter. J. Geophys. R., 119(7), 4168-4184, doi:10.1002/2013JC009705.

Mathiot, P., C. K. Beatty, T. Fichefet, H. Goosse, F. Massonnet, and M. Vancoppenolle, 2012: Better constraints on the sea-ice state using global sea-ice data assimilation. Geosci. Model Dev., 5, 1501–1515, www.geosci-model-dev.net/5/1501/2012/, doi:10.5194/gmd-5-1501-2012.

Morison, J. H., C. E. Long, and M. D. Levine, 1985: Internal wave dissipation under sea ice. J. Geophys. Res., 90(C6), 11959-11966, doi:10.1029/JC090iC06p11959.

Nguyen, A., D. Menemenlis, and R. Kwok, 2009: Improved modeling of the Arctic halocline with a subgrid-scale brine rejection parameterization, J. Geophys. Res, 114, C11014, doi: 10.1029/2008JC005121.

—, 2011: Arctic ice-ocean simulation with optimized model parameters: Approach and assessment. J. Geophys. Res., 116, C04025, doi:10.1029/2010JC006573.

Oke, P. R., G. B. Brassington, D. A. Griffin, and A. Schiller, 2008: The Bluelink ocean data assimilation system (BODAS). Ocean Modelling, 21, 46-70, doi: 10.1016/j.ocemod.2007.11.002.

Rampal, P., J. Weiss, and D. Marsan, 2009: Positive trend in the mean speed and deformation rate of Arctic sea ice, 1979-2007, J. Geophys. R., 114(C5), doi:10.1029/2008JC005066.

Rampal, P., Weiss, J., Dubois, C., Campin, J.M., 2011: IPCC climate models do not capture Arctic sea ice drift acceleration: Consequences in terms of projected sea ice thinning and decline. J. Geophys. Res., 116, 10.1029/2011JC007110.

Rampal, P., Bouillon, S., Ólason, E., and Morlighem, M., 2016: neXtSIM: a new Lagrangian sea ice model, The Cryosphere, 10, 1055-1073, doi:10.5194/tc-10-

1055-2016.

Reul, N., J. Tenerelli, J. Boutin, B. Chapron, F. Paul, E. Brion, F. Gaillard, and O. Archer, 2012: Overview of the first SMOS sea surface salinity products. Part I: Quality assessment for the second half of 2010, IEEE Trans. Geosci. Remote Sens., 50(5), 1636–1647, doi:10.1109/TGRS.2012.2188408.

Reynolds, R., and T. Smith, 1994: Improved global sea surface temperature analyses using optimum interpolation. J. Climate, 7, 929-948, DOI: http://dx.doi.org/10.1175/1520-0442(1994)007<0929:IGSSTA>2.0.CO;2.

Roemmich, D., J. Church, J. Gilson, D. Monselesan, P. Sutton, and S. Wijffels, 2015: Unabated planetary warming and its ocean structure since 2006. *Nature Climate Change* 5, 240–245. doi:10.1038/nclimate2513

Rothrock, D.A. and M. Wensnahan, 2007: The accuracy of sea-ice drafts measured from U. S. Navy submarines. J. Atmos. Oceanic Technol. doi:10.1175/JTECH2097.1.

Rothrock, D. A., D. B. Percival, and M. Wensnahan, 2008: The decline in arctic sea-ice thickness: Separating the spatial, annual, and interannual variability in a quarter century of submarine data, J. Geophys. Res., 113, C05003, doi:10.1029/2007JC004252.

Sakov, P. and P. R. Oke, 2008: A deterministic formulation of the ensemble Kalman _lter: an alternative to ensemble square root filters. Tellus A, 60(2):361-371, doi: 10.1111/j.1600-0870.2007.00299.x.

Sakov, P., F. Counillon, L. Bertino, K. A. Lisæther, P. R. Oke, and A. Korablev, 2012: TOPAZ4: an ocean-sea ice data assimilation system for the North Atlantic and Arctic. Ocean Science, 8:633-656, doi:10.5194/os-8-633-2012.

Samuelsen, A., C. Hansen, and H. Wehde, 2015: Tuning and assessment of the HYCOM-NORWECOM V2.1 biogeochemical modeling system for the North Atlantic and Arctic oceans. Geosci. Model Dev., 8(7), 2187-2202, DOI: 10.5194/gmd-8-2187-2015.

Ocean Sci. Discuss., doi:10.5194/os-2016-38, 2016
Manuscript under review for journal Ocean Sci.
Published: 27 June 2016

Schweiger, A., R. Lindsay, J. L. Zhang, M. Steele, H. Stern, and R. Kwok, 2011: Uncertainty in modeled Arctic Sea Ice volume, J. Geophys. Res., 116, C00D06, doi:10.1029/2011JC007084.

Schweiger, A. J., and J. Zhang, 2015: Accuracy of short-term sea ice drift forecasts using a coupled ice-ocean model, J. Geophys. Res., doi: 10.1002/2015jc011273.

Shimada, K., T. Kamoshida, M. Itoh, S. Nishino, E. Carmack, F. McLaughlin, S. Zimmermann, and A. Proshutinsky, 2006: Pacific Ocean inflow: Influence on catastrophic reduction of sea ice cover in the Arctic Ocean, Geophys. Res. Lett., 33(8), doi:10.1029/2005GL025624.

Simmons, A., S. Uppala, D. Dee, and S. Kobayashi, 2007: ERA-Interim: New ECMWF reanalysis products from 1989 onwards, ECMWF Newsletter, 110, 25-35.

Simon, E., A. Samuelsen, L. Bertino, and S. Mouysset, 2015: Experiences in multiyear combined state-parameter estimation with an ecosystem model of the North Atlantic and Arctic Oceans using the Ensemble Kalman Filter. J. Marine Sys., 152, 1-17, dio: 10.1016/j.jmarsys.2015.07.004.

Spreen, G., R. Kwok, and D. Menemenlis. 2011: Trends in Arctic sea ice drift and role of wind forcing: 1992-2009, Geophysical Research Letters, 38(19), doi: 10.1029/2011GL048970.

Stark, J., C. Donlon, M. Martin, and M. McCulloch, 2007: OSTIA: An operational, high resolution, real time, global sea surface temperature analysis system, in OCEAN 2007-Eurrope, pp. 1-4, IEEE, doi: 10.1109/OCEANSE.2007.4302251.

Steele, M., R. Morley, and W. Ermold, 2001: PHC: A global ocean hydrography with a high-quality Arctic Ocean, J. Climate, 14, 2079–2087, Doi:http://dx.doi.org/10.1175/1520-0442(2001)014<2079:PAGOHW>2.0.CO:2.

Tian-Kunze, X., L. Kaleschke, N. Maaß, M. Mäkynen, N. Serra, M. Drusch, and T. Krumpen, 2014: SMOS-derived sea ice thickness: algorithm baseline, product

specifications and initial verification, The Cryosphere, 8, 997-1018, doi:10.5194/tc-8-997-2014.

Tietsche, S., Notz, D., Jungclaus, J. H., and Marotzke, J., 2013: Assimilation of sea-ice concentration in a global climate model – physical and statistical aspects. Ocean Sci., 9, 19-36, doi: 10.5194/os-9-19-2013.

Wadhams, P. and R. J. Horne. 1980: An analysis of ice profiles obtained by submarine in the Beaufort Sea. J. Glaciol., 25, 401-424.

Wensnahan, M. and D. A. Rothrock, 2005: Sea-ice draft from submarine-based sonar: Establishing a consistent record from analog and digitally recorded data. Geophys. Res. Lett., 32, L11502, doi:10:1029/2005GL022507.

Wingham, D., C. Francis, S. Baker, C. Bouzinac, et al, 2006: CryoSat: A mission to determine the fluctuations in Earth's land and marine ice fields, Adv. Space Res., 37, 841–871, doi:10.1016/j.asr.2005.07.027.

Woodgate, R., K. Aagaard, and T. Weingartner, 2005: Monthly temperature, salinity, and transport variability of the Bering Strait through flow. Geophysical Research Letters, 32, L04601, DOI: 10.1029/2004GL021880.

Xie, J., F. Counillon, J. Zhu, J., and L. Bertino, 2011: An eddy resolving tidal-driven model of the South China Sea assimilating alongtrack SLA data using the EnOI, Ocean Sci., 7, 609–627, doi:10.5194/os-7-609-2011.

Zygmuntowska, M., P. Rampal, N. Ivanova, and L. H. Smedsrud, 2014: Uncertainties in Arctic sea ice thickness and volume: new estimates and implications for trends. The Cryosphere, 8, 705-720, doi:10.5194/tc-8-705-2014.

Ocean Sci. Discuss., doi:10.5194/os-2016-38, 2016
Manuscript under review for journal Ocean Sci.
Published: 27 June 2016

Ocean Science
Discussions
Open Access
EGU

Table 1. Overview of assimilated observations per cycle, average numbers for the cycles during which the observations are present. (1) The resolution of ice concentration product increased to 10 km. Unless specified, all observations from http://marine.copernicus.eu

Type	Number	After SO	Spacing	Resolution	Period	Provider
SLA	$9x10^4$	$4x10^4$	Track	7 km	1992-2013	CLS
SST	$6x10^3$	$6x10^3$	Gridded	100 km	1990-1998	Reynolds SST from NCDC (http://www.nhc.noaa.gov/aboutsst.shtml)
SST	$2x10^6$	$2.4x10^5$	Gridded	5 km	1998-2013	OSTIA from UK Met Office
In-situ T/S	$3x10^4$	$5x10^3$	Point	-	1990-2013	Ifremer + other
ICEC (SSM/I)	$9x10^4$	$5x10^4$	Gridded	25 km	1990-2002	OSISAF
ICEC (AMSR-E)	$1.6x10^5$	$5x10^4$	Gridded	12.5 km(1)	2002-2013	OSISAF
ICEC (AMSR-E)	$1.6x10^5$	$5x10^4$	Gridded	12.5 km	2008-2009	AMSR-E (http://nsidc.org/data/amsre/)
Ice drift (CERSAT)	$5x10^3$	$5x10^3$	Gridded	62.5 km	2002-2010	Ifremer
Ice drift (OSISAF)	$5x10^3$	$5x10^3$	Gridded	62.5 km	2011-2013	OSISAF
Total	$2.3x10^6$	$4x10^5$				

Ocean Sci. Discuss., doi:10.5194/os-2016-38, 2016
Manuscript under review for journal Ocean Sci.
Published: 27 June 2016

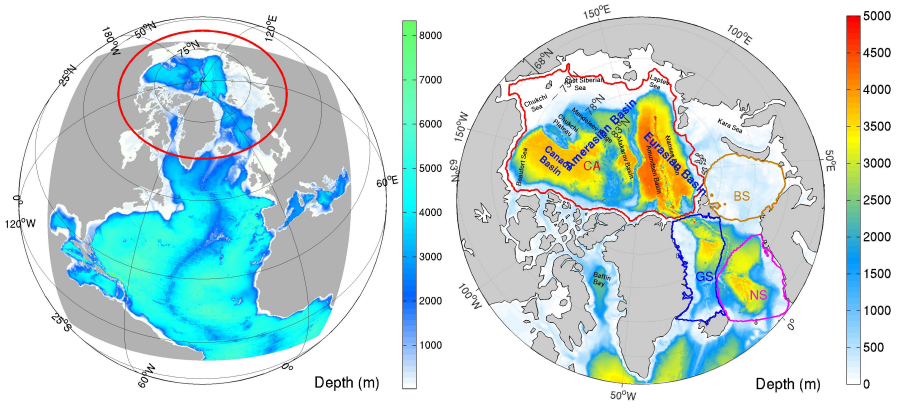

Fig 1. **Left**: Bottom topography in the whole TOPAZ4 domain. The red line delimits the Pan-Arctic region north of 63°N. **Right**: Definition of sub-basins and marginal seas. The domain is divided into the four sub-regions delimits by the colored lines: the Central Arctic in red (CA), the Greenland Sea in blue (GS), the Barents Sea in orange (BS), and the Norwegian Sea in magenta (NS).

Ocean Sci. Discuss., doi:10.5194/os-2016-38, 2016
Manuscript under review for journal Ocean Sci.
Published: 27 June 2016

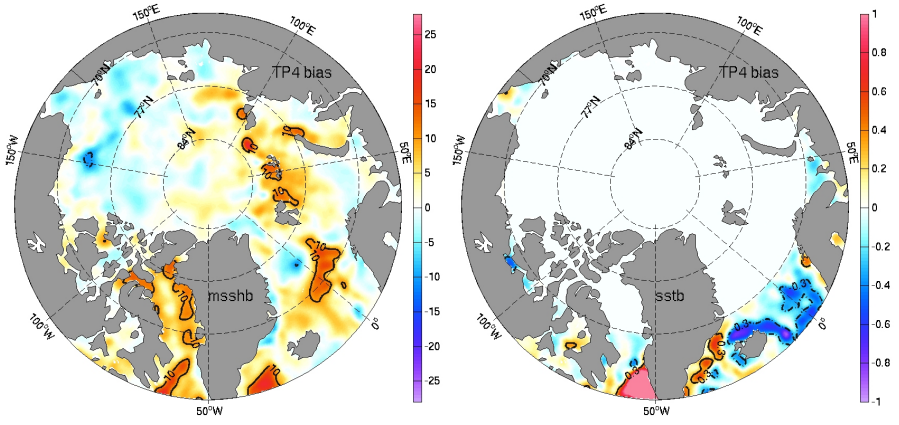

Fig 2. Estimates of the mean SSH bias (**Left**) and the SST bias (**Right**) obtained at last analyzed date by online parameter estimation. In the left panel, the solid (dashed) line indicates the 10 (-10) cm isolines. In the right panel, the solid (dashed) line indicates the 0.3 °C (-0.3 °C) isolines. There is no bias estimation for SST in the white area north of 70°N.

Ocean Sci. Discuss., doi:10.5194/os-2016-38, 2016
Manuscript under review for journal Ocean Sci.
Published: 27 June 2016

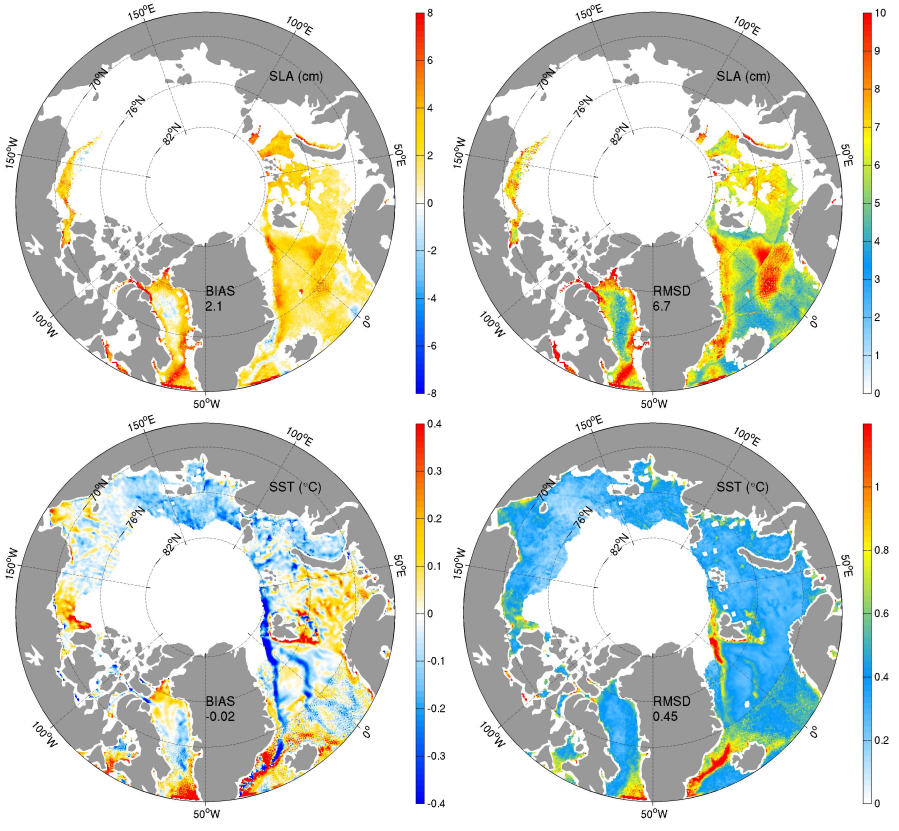

Fig 3. **Top**: Residual bias (left) and RMSD (right) between the daily average SLA from the reanalysis and the assimilated along-track SLA data averaged over the period 1993-2013 (unit: cm). **Bottom**: The corresponding residual bias (left) and RMSD (right) between the daily average SST from the reanalysis and the assimilated observations averaged over the period 1999-2013 (unit: °C). Areas with less than 30 observations have been masked in white.

Ocean Sci. Discuss., doi:10.5194/os-2016-38, 2016
Manuscript under review for journal Ocean Sci.
Published: 27 June 2016

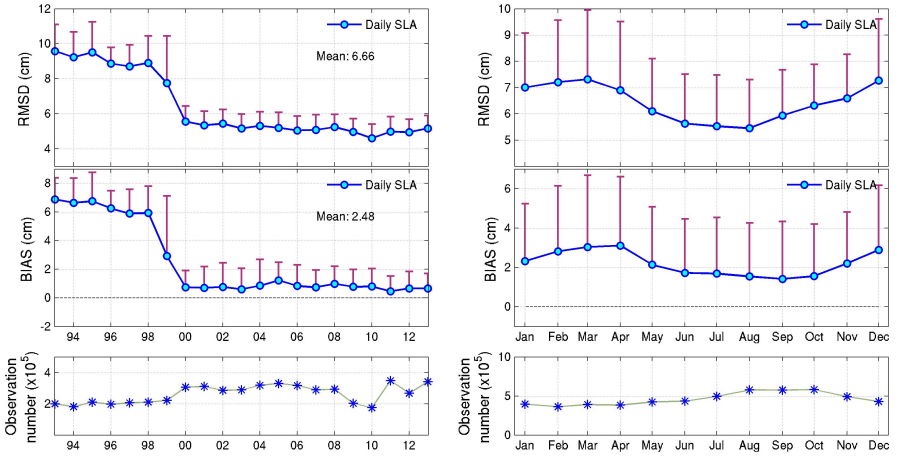

Fig 4. **Left**: Yearly averaged estimates of daily SLA RMSD (upper) and the residual bias (middle) of the TOPAZ reanalysis calculated against the along-track SLA available in the Pan-Arctic region (unit: cm). The error bars denote the standard deviations of the daily statistics within each year. The bottom panel is the number of available observations in each year. **Right**: Similar plot for monthly averaged estimate of daily SLA RMSD (upper), and the residual bias (middle). The error bars denote the standard deviations of the daily statistic within each month. The bottom panel shows the number of observations available for each month in the Pan-Arctic during 1993-2013.

Ocean Sci. Discuss., doi:10.5194/os-2016-38, 2016
Manuscript under review for journal Ocean Sci.
Published: 27 June 2016

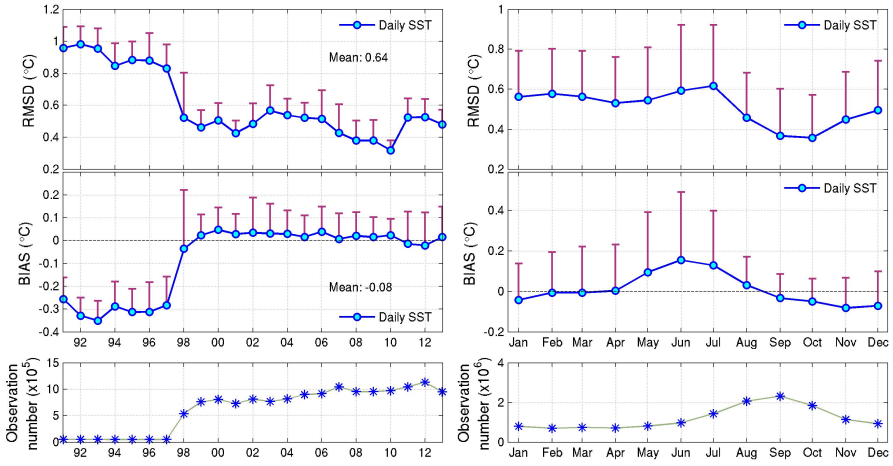

Fig 5. Same as the previous figure but for SST for the period 1991-2013 (unit: °C).

Ocean Sci. Discuss., doi:10.5194/os-2016-38, 2016
Manuscript under review for journal Ocean Sci.
Published: 27 June 2016

Ocean Science
Discussions
Open Access
EGU

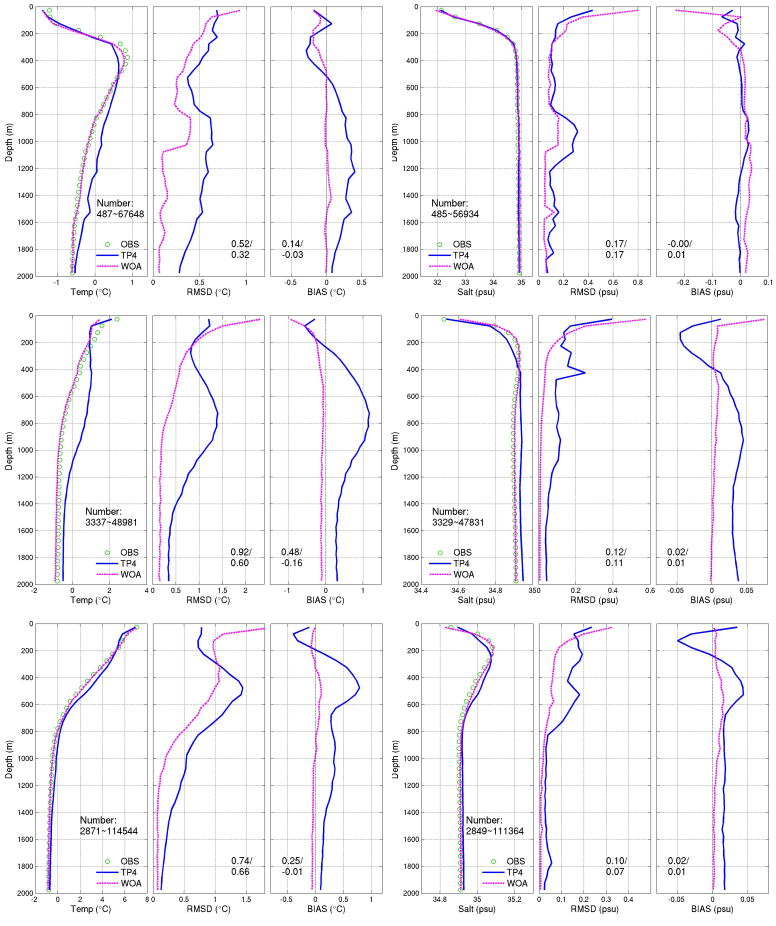

1 Central Arctic

2 Greenland Sea

3 Norwegian Sea

Ocean Sci. Discuss., doi:10.5194/os-2016-38, 2016
Manuscript under review for journal Ocean Sci.
Published: 27 June 2016

Ocean Science
Discussions
Open Access
EGU

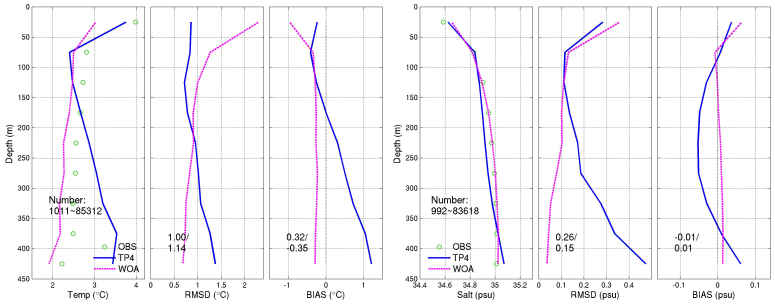

Barents Sea

Fig 6. The mean profiles of temperature (*left*) and salinity (*right*) and the corresponding bias and RMSD in each of the marginal seas of the Pan-Arctic region. The green circle is the observations, the blue lines are the TOPAZ reanalysis, and the pink lines are from the WOA13 climatology. The numbers in the first-column subpanels are the minimal and maximal number of observations available in each of 50 m depths; the upper numbers in the other-column subpanels are the mean estimate in vertical for TOPAZ reanalysis, and the lower numbers is for WOA13.

Ocean Sci. Discuss., doi:10.5194/os-2016-38, 2016
Manuscript under review for journal Ocean Sci.
Published: 27 June 2016

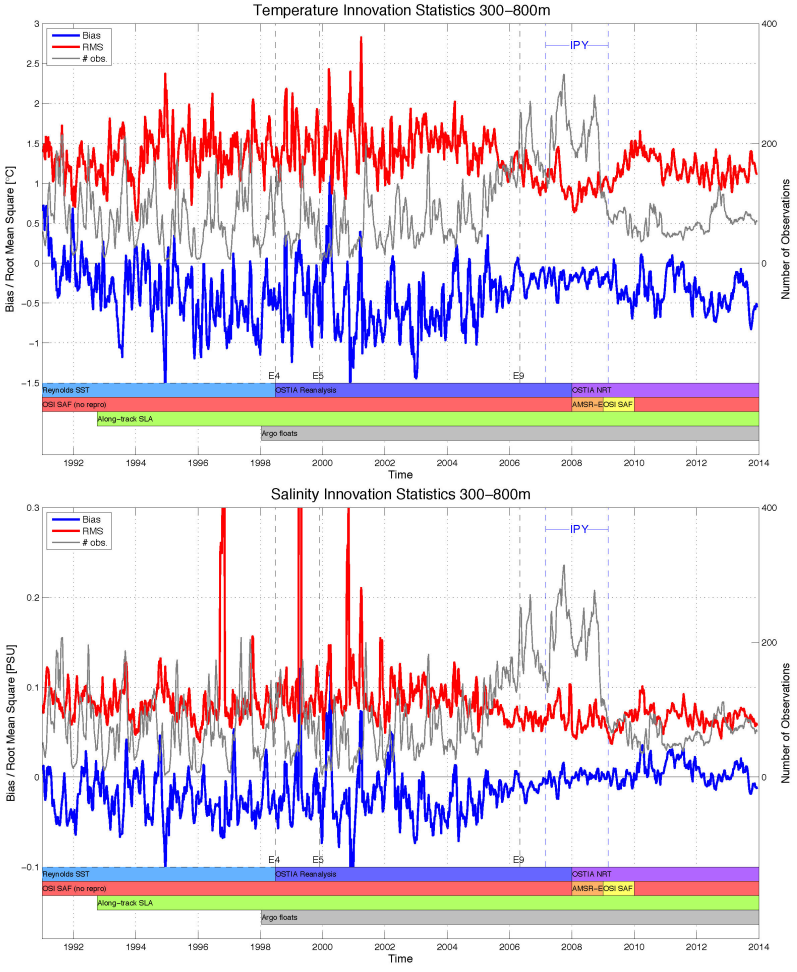

Fig 7. Time series of innovation statistics for temperature (**top**) and salinity (**bottom**) observed at the depth of between 300-800 m depths. The bias is plotted with a blue line, the RMSD is in red and the number of assimilated observations is plotted with a grey line. The time series are filtered with a 28 days moving window. The vertical dashed lines indicate the major change events in the course of the TOPAZ reanalysis.

Ocean Sci. Discuss., doi:10.5194/os-2016-38, 2016
Manuscript under review for journal Ocean Sci.
Published: 27 June 2016

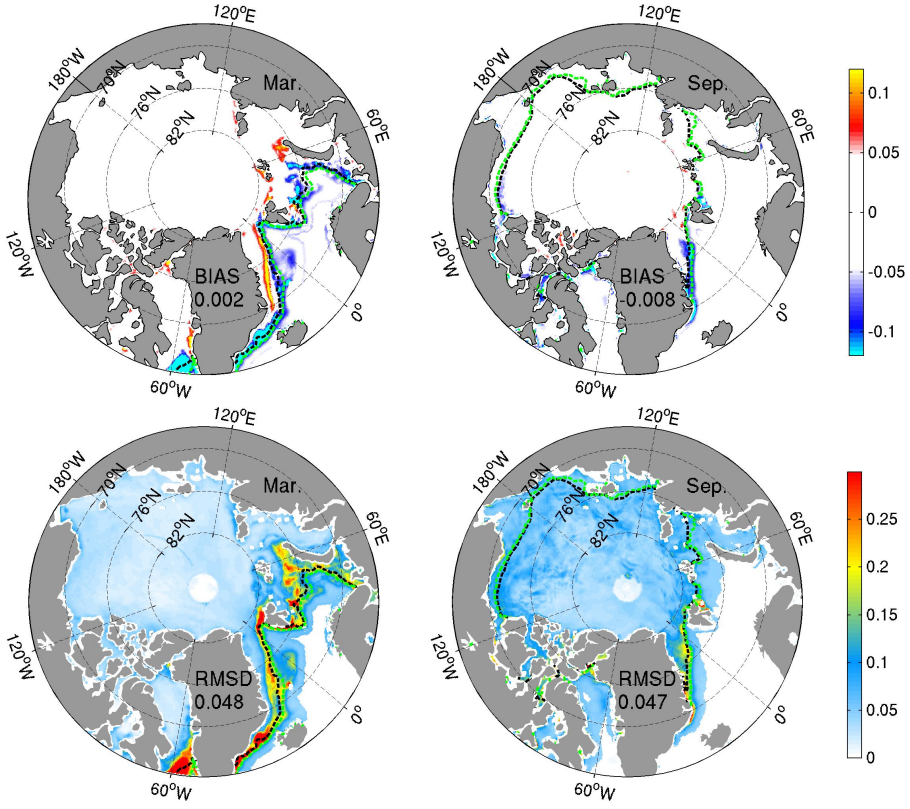

Fig 8. Spatial bias (upper) and RMSD (lower) of sea ice concentration in the TOPAZ reanalysis for March (*left*) and September (*right*) calculated from the daily averages for the period 1991-2013. The dashed black (green) lines delimit the monthly mean sea ice edges (at 15%) in the TOPAZ reanalysis (OSISAF).

Ocean Sci. Discuss., doi:10.5194/os-2016-38, 2016
Manuscript under review for journal Ocean Sci.
Published: 27 June 2016

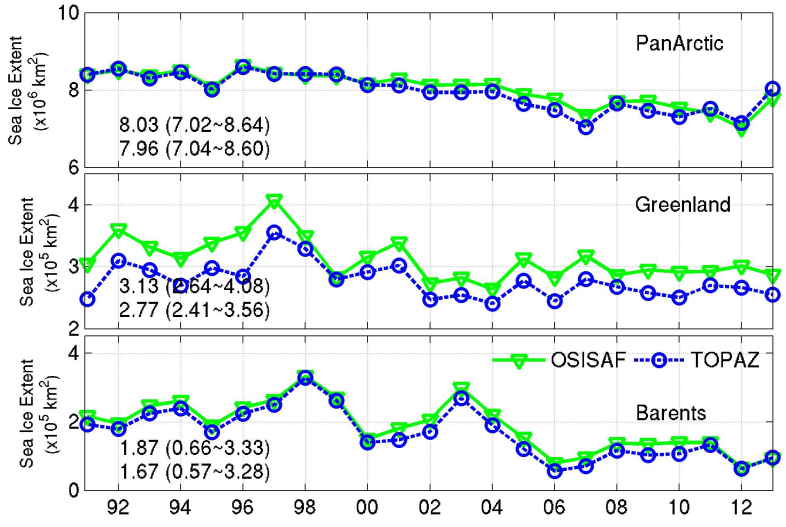

Fig 9. Yearly time series of the sea ice extent in the Pan-Arctic region, the Greenland Sea, and the Barents Sea from TOPAZ reanalysis (dashed) and OSISAF (solid).

Ocean Sci. Discuss., doi:10.5194/os-2016-38, 2016
Manuscript under review for journal Ocean Sci.
Published: 27 June 2016

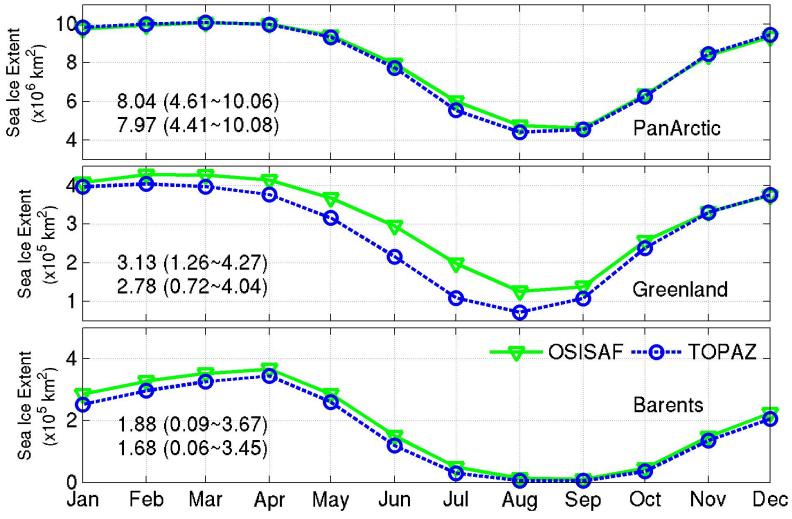

Fig 10. Seasonality of the sea ice extents in the TOPAZ reanalysis (blue line) and OSISAF (green line) in the Pan-Arctic Ocean, Greenland Sea, and Barents Sea regions.

Ocean Sci. Discuss., doi:10.5194/os-2016-38, 2016
Manuscript under review for journal Ocean Sci.
Published: 27 June 2016

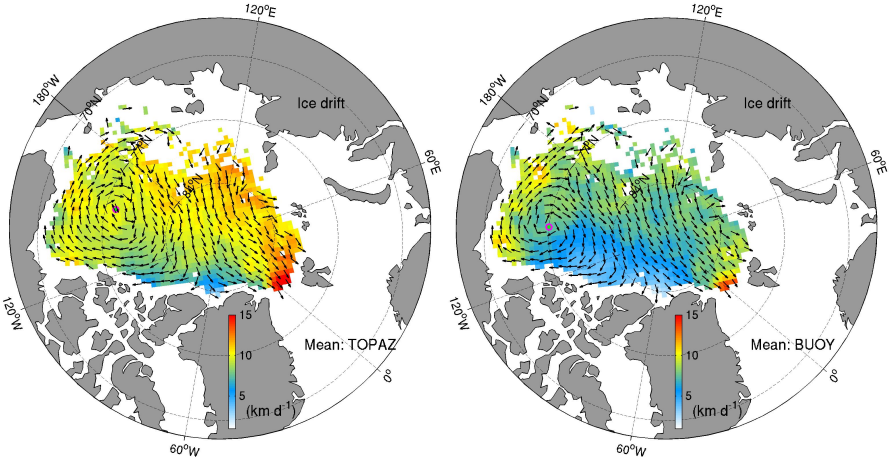

Fig 11. Sea ice drift vectors (*arrows*) and speeds (*color shading*) averaged over the period 1991-2011 for (a) TOPAZ reanalysis and (b) IABP buoys. The center of the anticyclonic Beaufort Gyre is marked with a magenta circle at (155°W, 78.1°N) in the TOPAZ reanalysis and (145°W, 77°N) in the observations respectively.

Ocean Sci. Discuss., doi:10.5194/os-2016-38, 2016
Manuscript under review for journal Ocean Sci.
Published: 27 June 2016

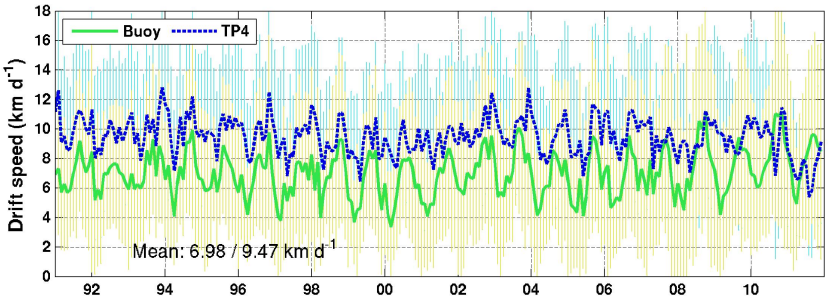

Fig 12. Monthly time series of the daily averaged sea ice drift speeds in the Central Arctic from the TOPAZ reanalysis (blue line) and the IABP buoys (green line) during 1991-2011. The error bars represent the standard deviations of the daily estimates for each month.

Ocean Sci. Discuss., doi:10.5194/os-2016-38, 2016
Manuscript under review for journal Ocean Sci.
Published: 27 June 2016

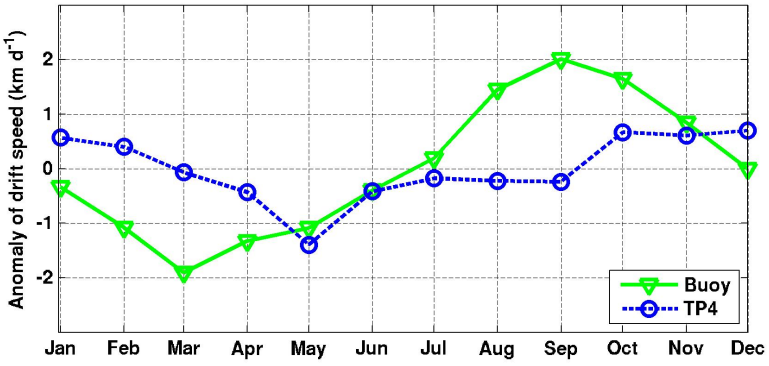

Fig 13. Seasonality of the sea ice drift velocities from the reanalysis and the buoy during 1991-2011.

Ocean Sci. Discuss., doi:10.5194/os-2016-38, 2016
Manuscript under review for journal Ocean Sci.
Published: 27 June 2016

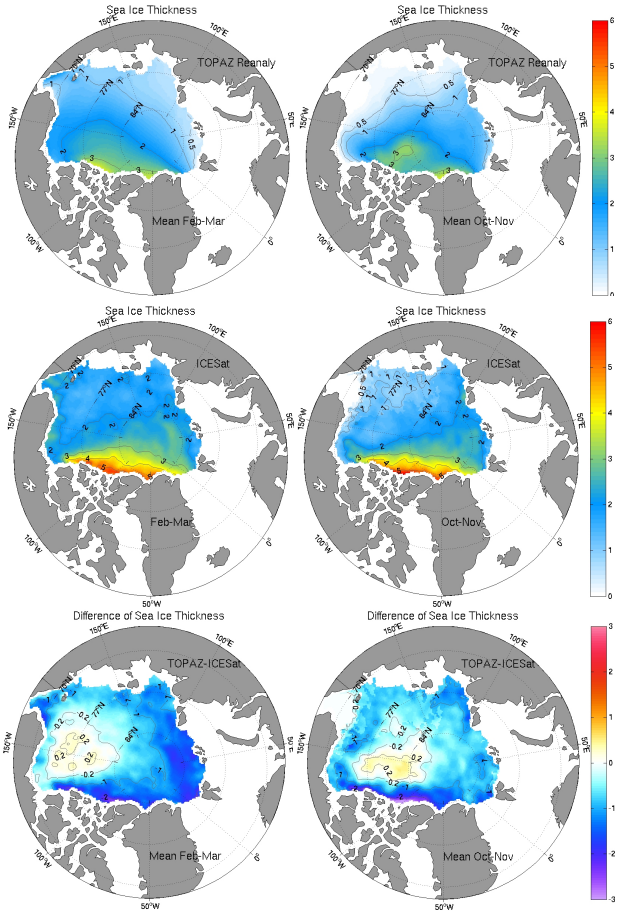

Fig 14. Mean sea ice thicknesses from TOPAZ (upper) and ICESat (middle), and their difference (bottom) for February-March (*in left column*) and October-November (*in right column*) averaged over the period 2003-2008.

Ocean Sci. Discuss., doi:10.5194/os-2016-38, 2016
Manuscript under review for journal Ocean Sci.
Published: 27 June 2016

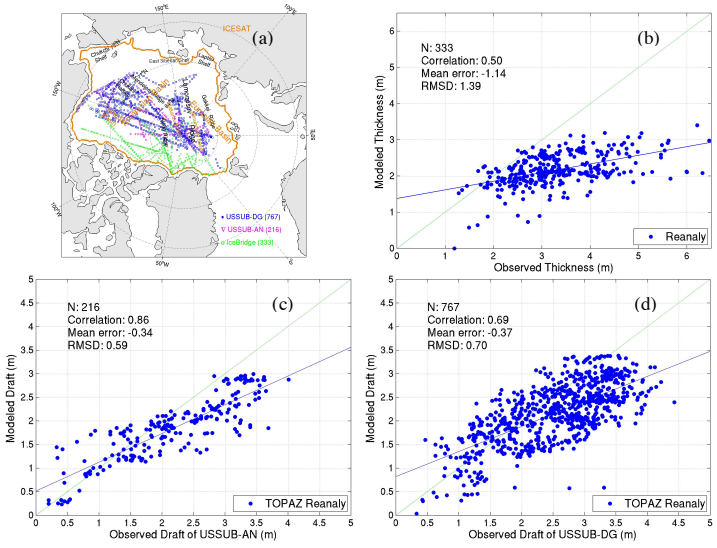

Fig 15. Validation the sea ice thickness in the TOPAZ reanalysis versus available in situ observations. (a) Locations of in situ observations available from IceBridge, USSUB-AN and USSUB-DG in the Central Arctic. Regression analysis of TOPAZ reanalysis (b) vs. IceBridge; (c) vs. USSUB-AN; (d) vs. USSUB-DG.

Ocean Sci. Discuss., doi:10.5194/os-2016-38, 2016
Manuscript under review for journal Ocean Sci.
Published: 27 June 2016

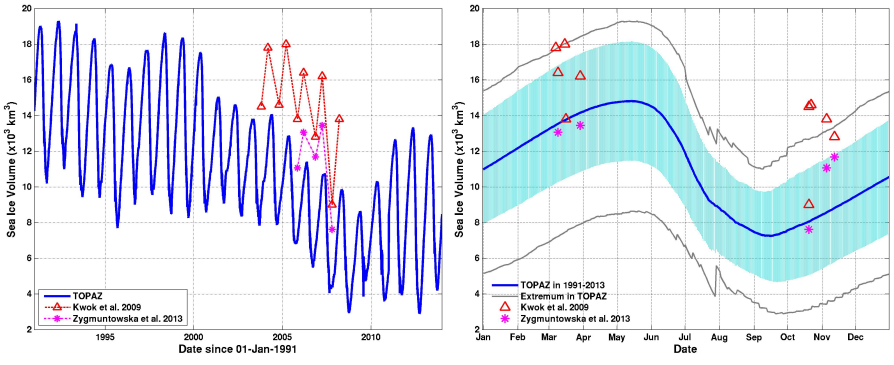

Fig 16. **Left**: Time series of the daily averaged sea ice volume in the Arctic from the TOPAZ4 (blue line) and the observations from Kwok et al. (2009) and from Zygmuntowska et al. (2013). **Right**: Daily time series of the averaged sea ice volume in the Arctic from the TOPAZ4 for the period 1991-2013 (blue line) and the standard deviation shown as the cyan error-bar. The gray lines represent the extreme volumes in the 23 years. The triangle and start markers are the observations estimated by Kwok et al. (2009) and Zygmuntowska et al. (2013) respectively.

Ocean Sci. Discuss., doi:10.5194/os-2016-38, 2016
Manuscript under review for journal Ocean Sci.
Published: 27 June 2016

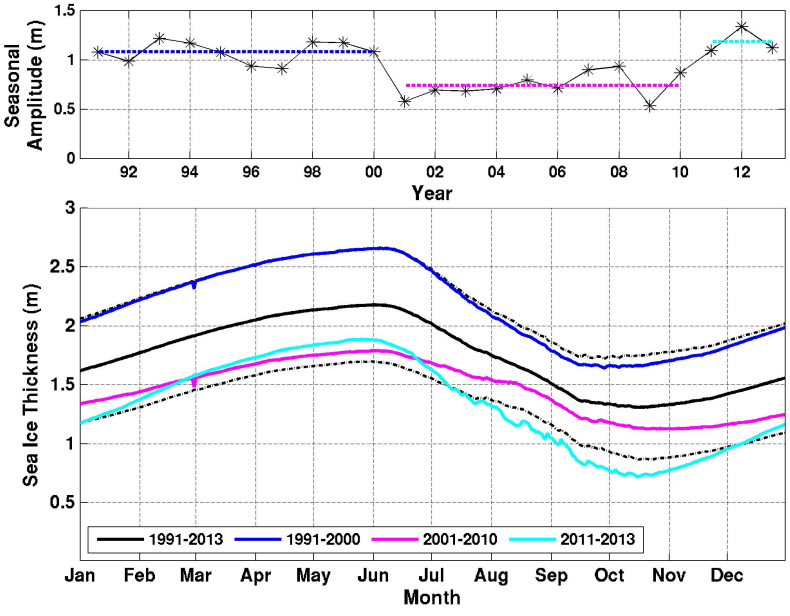

Fig 17. **TOP**: Yearly time series of the seasonal amplitudes of the mean sea ice thickness in the Central Arctic with the solid black line. The dashed lines represent the averaged estimate for: 1991-2000, 2001-2010, and 2011-2013 (1.08, 0.74, and 1.18 m respectively). **Bottom**: Daily time series of the mean sea ice thickness in the Central Arctic for three different time periods. The black dashed lines denote the standard deviation for the 23 yearly estimates.